Original article

Simulation of the oxidative metabolization pattern of netupitant, an NK$_1$ receptor antagonist, by electrochemistry coupled to mass spectrometry

Ruxandra Chira [a, 1], Jens Fangmeyer [b, 1], Ioan O. Neaga [a], Valentin Zaharia [c], Uwe Karst [b, **], Ede Bodoki [a, *], Radu Oprean [a]

[a] Analytical Chemistry Department, "Iuliu Haţieganu" University of Medicine and Pharmacy, 400349, Cluj-Napoca, Romania
[b] University of Münster, Institute of Inorganic and Analytical Chemistry, 48149, Münster, Germany
[c] Organic Chemistry Department, "Iuliu Haţieganu" University of Medicine and Pharmacy, 400012, Cluj-Napoca, Romania

ARTICLE INFO

ABSTRACT

Considering the frequent use of netupitant in polytherapy, the elucidation of its oxidative metabolization pattern is of major importance. However, there is a lack of published research on the redox behavior of this novel neurokinin-1 receptor antagonist. Therefore, this study was performed to simulate the intensive hepatic biotransformation of netupitant using an electrochemically driven method. Most of the known enzyme-mediated reactions occurring in the liver (i.e., N-dealkylation, hydroxylation, and N-oxidation) were successfully mimicked by the electrolytic cell using a boron-doped diamond working electrode. The products were separated by reversed-phase high-performance liquid chromatography and identified by high-resolution mass spectrometry. Aside from its ability to pinpoint formerly unknown metabolites that could be responsible for the known side effects of netupitant or connected with any new perspective concerning future therapeutic indications, this electrochemical process also represents a facile alternative for the synthesis of oxidation products for further in vitro and in vivo studies.

© 2021 Xi'an Jiaotong University. Production and hosting by Elsevier B.V. This is an open access article under the CC BY-NC-ND license (http://creativecommons.org/licenses/by-nc-nd/4.0/).

1. Introduction

The quality of life of patients has been a major area of concern over the last decades, with efforts made to improve the palliative care of individuals with terminal illnesses or to relieve the side effects associated with chemotherapy protocols. Netupitant, a relatively new and selective neurokinin-1 (NK$_1$) receptor antagonist, is used either in monotherapy or in combination with palonosetron (a 5-HT$_3$ receptor antagonist) for the control of unwanted side effects (e.g., nausea and emesis) associated with the postoperative condition or those caused by acute and delayed chemotherapy [1–4]. Given the wide distribution of the NK$_1$ receptors throughout the central and peripheral nervous systems and the omnipresence of the substance P (SP) peptide in all bodily fluids, a better understanding of the SP/NK$_1$ receptor system is warranted to add to our understanding of how these molecules contribute to the molecular bases of numerous human pathologies, as suggested by Huang and Korlipara [5] and Muñoz and Coveñas [6].

Netupitant, a potent non-peptide, contains two trifluoromethyl groups on its phenyl ring, which according to Pertusati et al. [7] is essential for the good penetration of the molecule into the nervous system as well as its pharmacological activity and intensive biotransformation. As described by Curran et al. [8], netupitant is a moderate enzyme inhibitor that is rapidly absorbed and extensively metabolized through phase I and II reactions in the liver. It is then cleared from the body via the hepatobiliary excretion system [9,10]. Besides the conventional in vivo and in vitro approaches, electrochemistry (EC) coupled to a separation technique, such as liquid chromatography (LC), followed by the detection and identification of the electrochemically generated metabolites by mass spectrometry (MS), represents a third and purely instrumental way to investigate the metabolic pathways of new pharmaco-active

agents, such as netupitant [11,12]. In the last decades, EC/LC/MS has grown to be a powerful tool, especially in the simulation of phase I metabolic reactions, which are typically catalyzed by enzymes of the cytochrome P450 (CYP) superfamily [13,14]. The LC separation of the electrochemically generated metabolites frequently provides new information regarding the formation of isomers that would otherwise go undetected, such as the organoarsenic metabolite generated from electrochemically oxidized roxarsone in a study by Frensemeier et al. [15]. Several metabolization studies have revealed a good correlation between enzymatically and electrochemically oxidized pharmaceuticals [16–18]. Moreover, electrochemically mimicked reactions, such as hydroxylation, dehydrogenation, and N-/O-dealkylation, have been reported [12,19,20].

Given that there is a complete lack of information regarding the electrochemical behavior of netupitant, this study was carried out to evaluate the similarities between the electrochemically generated species of the enzyme inhibitor and its previously reported metabolites, some of which had already been proven in a study by Spinelli et al. [10] to have pharmacological activity. Formerly unknown metabolites may also be responsible for the undesired side effects associated with netupitant treatment, such as headache, constipation, and electrocardiogram abnormalities [21,22], and may be correlated with new therapeutic indications currently under extensive study [5,21,23].

Filling the knowledge gaps in the metabolization pattern of this novel NK_1 receptor antagonist is of high importance for its good pharmacovigilance. Thus, EC/LC/MS was applied as a hyphenated analytical tool for mimicking the phase I metabolization of netupitant, detecting its formerly unknown intermediates, and enabling alternative routes for the synthesis of potentially novel or already established metabolites.

2. Experimental

2.1. Reagents and chemicals

Netupitant was purchased from Shanghai Seebio Biotech, Inc. (Shanghai, China). Ammonium formate (≥99.0%, for HPLC), ammonia solution (25%), and formic acid (99%) were obtained from Sigma-Aldrich (Steinheim, Germany) and Th. Geyer GmbH & Co. KG (Renningen, Germany). LC/MS-grade acetonitrile (ACN) was purchased from Merck (Darmstadt, Germany). Working solutions of netupitant (10 μM) were prepared by diluting a 1 mM stock
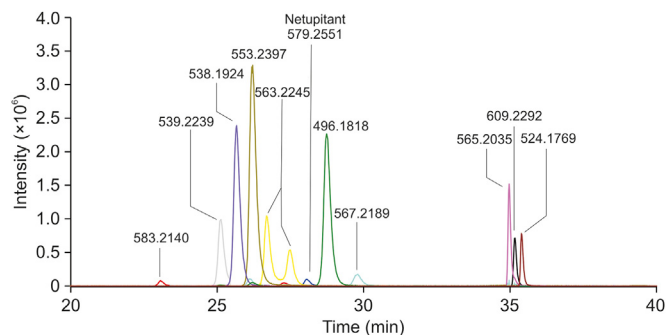

Fig. 2. Extracted ion chromatograms of the electrochemically generated oxidation species (*m/z* 583.2140, *m/z* 539.2239, *m/z* 538.1924, *m/z* 553.2397, *m/z* 563.2245, *m/z* 496.1818, *m/z* 567.2189, *m/z* 565.2035, *m/z* 609.2292, and *m/z* 524.1769) of netupitant (*m/z* 579.2551) at 1700 mV.

solution (prepared in ACN) with 10 mM ammonium formate buffer. The working solutions were adjusted to three different pH values by combining them respectively with 10 mM ammonium formate buffers of pH 3.0, 7.4, and 9.0 that had been mixed with ACN at a 50/50 (*V/V*) ratio. Double-distilled water generated with an Aquatron A4000D water purification system (Cole-Parmer, Staffordshire, UK) was used for all sample preparations.

2.2. Online EC coupled to MS

For the electrochemical oxidation of netupitant, the different working solutions were passed through a thin-layer flow-through electrochemical cell (μ-PrepCell 2.0, Antec Scientific, Zoeterwoude, The Netherlands) via a syringe pump (Model 74900, Cole-Parmer, Staffordshire, UK) set at a flow rate of 15 μL/min. The electrochemical cell was equipped with a boron-doped diamond working electrode, a conductive polyetheretherketone counter electrode, and a Pd/H_2 reference electrode, with a homemade potentiostat used to ensure potentiostatic control. All reported potentials were expressed with respect to the Pd/H_2 reference electrode. To investigate the dependency of the potential on pH, it was increased from 0 to 2500 mV at a rate of 10 mV/s for each of the three working solutions of different pH values. The effluent outlet of the electrochemical cell was directly connected to the electrospray ionization (ESI) source of a high-resolution time-of-flight (ToF) mass spectrometer (microTOF, Bruker Daltonik, Bremen, Germany) operating in positive ionization mode in the range of 50–1300 a.m.u. Subsequently, the resulting mass spectra were plotted as three-dimensional mass voltammograms. The mass spectrometric parameters used are detailed in the Supplementary data (SI 1).

2.3. Offline EC coupled to LC and MS

On the basis of the data retrieved from the mass voltammograms, netupitant was oxidized at a constant potential (1700 mV vs. Pd/H_2) in all subsequent EC/LC/MS experiments, leading to a balanced yield of all oxidation products. The effluent from the electrolytic cell was collected in a vial and subsequently analyzed by LC/MS. A polar-embedded C_{18}-based LC column (ProntoSIL C_{18} ace-EPS, 100 mm × 2.0 mm, 3 μm, Bischoff Chromatography, Leonberg, Germany), which was attached to an LC system (Shimadzu, Duisburg, Germany) consisting of two LC-10ADVP pumps, a SIL-HTA autosampler, a DGU 14A degasser, a CTO-AVP column oven, and a CBM-20A controller, was used for separation of the products. The detection of netupitant and its metabolites was performed with a high-resolution microTOF mass spectrometer (Bruker
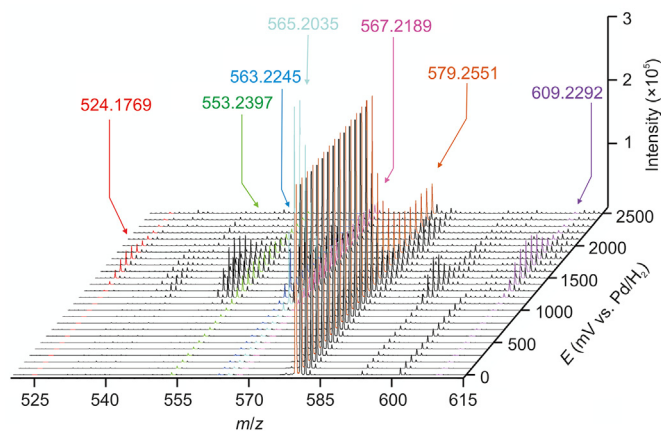

Fig. 1. Three-dimensional mass voltammogram (*m/z* 520–615) of netupitant (*m/z* 579.2551) and its oxidation products in the potential range of 0–2500 mV vs. Pd/H_2.
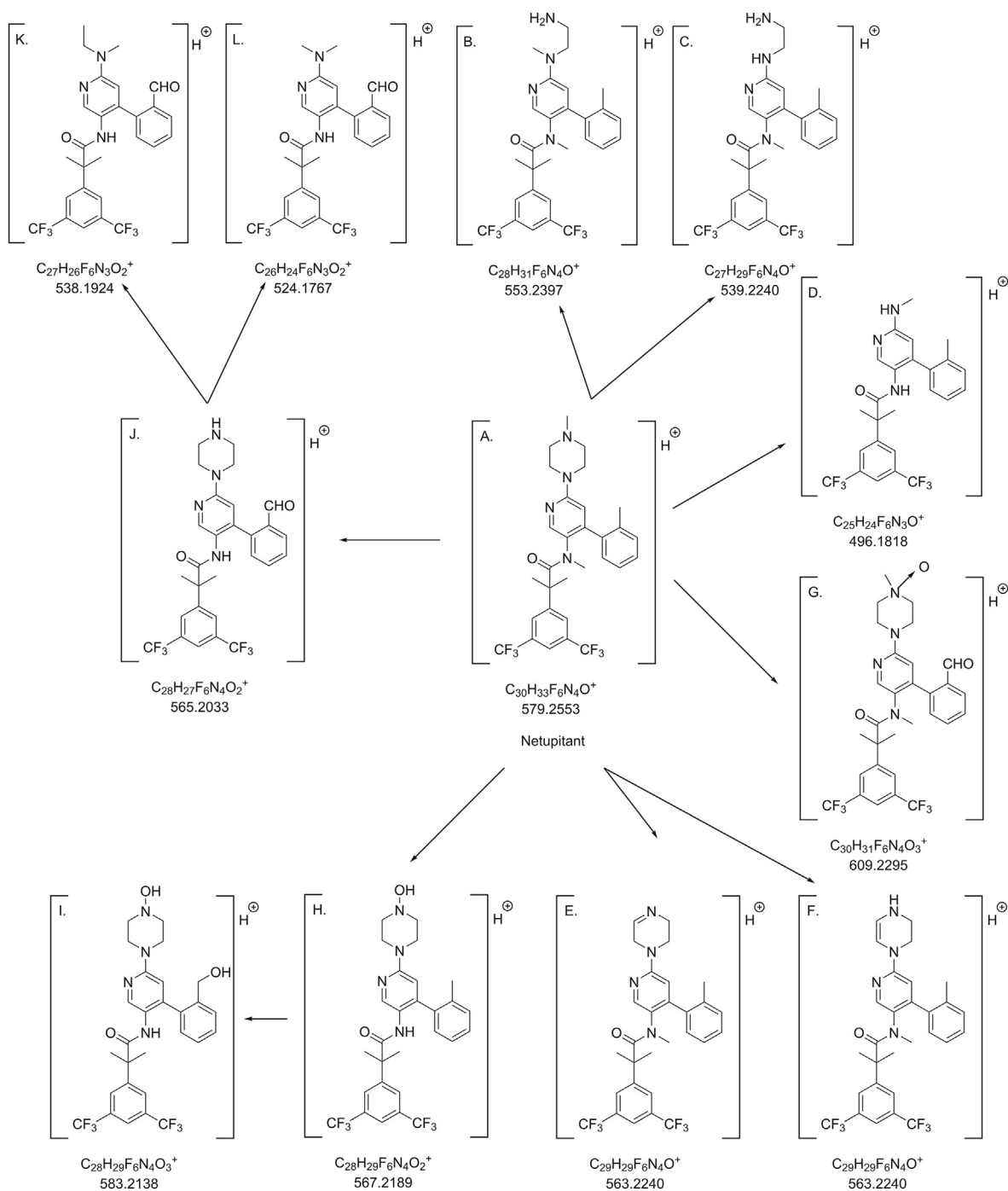
Fig. 3. Proposed structures of the electrochemically generated metabolites of netupitant.

Daltonik GmbH, Bremen, Germany). To gain further structural information on the molecules, fragmentation experiments were performed using the quadrupole ToF-based timsTOF fleX mass spectrometer (Bruker Daltonik GmbH, Bremen, Germany). The gradient profile employed and additional details of the LC and MS parameters used are given in the Supplementary data (SI 1–3).

The evaluation of possible structures related to the parent compound took into consideration of the calculated mass deviation between each structure and the detected *m/z* signal. The proposed structures had a lower than 1 ppm mass deviation, as presented in Tabel S1.

3. Results and discussion

The electrochemical behavior of netupitant at increasing potentials of the working electrode under different pH conditions was monitored by online coupling with the mass spectrometer. No significant pH-dependent changes (pH 3.0–9.0) were recorded in the EC/MS profile or in the efficiency of netupitant oxidation. Therefore, all subsequent measurements were performed at a physiological pH value of 7.4 (Fig. 1).

Following careful adjustment of the working electrode's potential so as to generate a balanced yield of all oxidation products
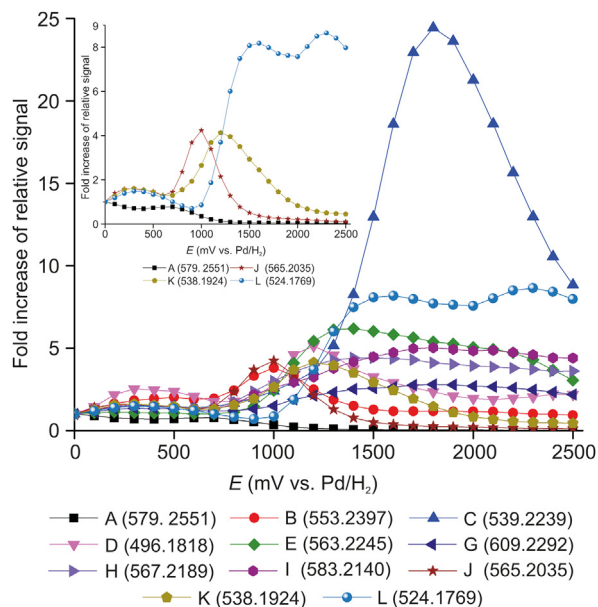
Fig. 4. Relative signals of the most relevant protonated ions of the electrochemically generated products of netupitant versus the applied potential. Inset: zoomed-in view of the relative signals of the protonated species resulting from the further electrochemical reactions undergone by the *N,N*-demethylated compound that had gone through a previous oxidation reaction with a carbonyl group (*m/z* 565.2035).

Fig. 5. MS/MS fragmentation pattern of netupitant (*m/z* 579.2551) at 28.5 min (compound A in Fig. 3).

with the EC/MS setup, the 10 μM netupitant working solution was oxidized at a constant potential of 1700 mV and subsequently analyzed by LC/MS. Considering the large number of electrochemical species that could be generated, the effluent collected from the electrolyzed netupitant sample was first separated by LC before MS identification of the products and their further fragmentation on a quadrupole ToF-based mass spectrometer. The extracted ion chromatograms of the parent compound and all major electrochemically generated species are presented in Fig. 2.

Netupitant had gone through various oxidation reactions within the electrochemical cell, such as hydroxylation and *N*-dealkylation. Additionally, at a given potential, some of the oxidation products underwent further hydroxylation, dehydrogenation, and dealkylation processes. The proposed structures of all electrochemically generated metabolites of netupitant are depicted in Fig. 3.

To obtain a more coherent overview of the subsequent redox steps occurring in a potential-dependent manner in the EC/MS
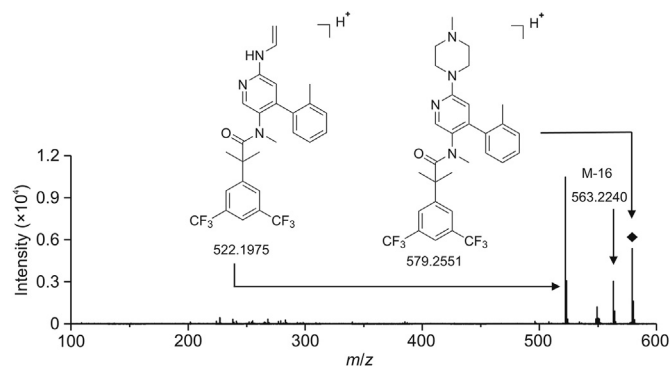
setup, the change in the relative MS signal of the recorded protonated molecular ions according to the applied potential was determined (Fig. 4). At approximately 700 mV, along with the simultaneous decrease in the relative signal of the parent compound (Fig. 3A), a signal increase was observed for *m/z* 553.2397 (Fig. 4), a product associated with a double *N*-dealkylation reaction of netupitant (Fig. 3B, *m/z* 553.2397). At approximately 1000 mV, the decrease in the signal intensity of the parent compound coincided with an increase in the relative signals of *m/z* 565.2035 and 567.2189 (Fig. 4). The most significant increase in the relative signal was observed for *m/z* 539.2239 (Fig. 3C), which along with *m/z* 553.2397 and 496.1818 (Figs. 3B and D) was associated with opening of the piperazine ring of netupitant. The mono *N*-demethylated product of netupitant, reported in the literature as one of its main metabolites [10], could not be detected in our study. Nevertheless, the formation of two isobaric compounds (*m/z* 563.2245) was observed, having been well separated by the EC/LC/MS setup (Fig. 2). These compounds were possibly derived from the subsequent dehydrogenation of the *N*-demethylated product. One possibility might be the formation of two positional isomers, the proposed structures of which are depicted in Fig. 3E and F. However, other isomerization points cannot be ruled out and will require future structural elucidation. The *N*-oxidation and hydroxylation of netupitant, followed by the oxidation of the newly attached hydroxyl group, led to the formation of *m/z* 609.2292 (Fig. 3G). The possible formation of an isobaric compound of structure G containing a carboxylic group instead of the aldehyde moiety has been ruled out, since it could not be detected in the

Table 1
Comparison between the reported phase I biotransformation of netupitant in vivo [10] and its electrochemically mimicked oxidation.

Observed reactions	In vivo biotransformation	Electrochemical oxidation	Observations regarding the present study
Mono *N*-demethylation	Yes	No	—
Dehydrogenation	No	Yes	Of mono *N*-demethylated compound
Bis *N*-demethylation	Yes	Yes	Of netupitant (*m/z* 563.2245, *m/z* 565.2035, *m/z* 567.2189, and *m/z* 583.2140)
Mono hydroxylation	Yes (of netupitant)	Yes	Of *N, N*-demethylated compound (*m/z* 567.2189)
Di-hydroxylation	Yes	Yes	Of *N, N*-demethylated compound (*m/z* 583.2140)
Oxidation to a carbonyl group	Yes	Yes	Of hydroxylated *N, N*-demethylated compound (*m/z* 565.2035)
		Yes	Of hydroxylated *N*-oxide compound (*m/z* 609.2295)
N-oxidation	Yes (of netupitant)	Yes	Of carbonyl netupitant (*m/z* 609.2295)
Piperazine degradation	Yes (intermediate metabolites)	Yes	Of netupitant (*m/z* 553.2392, *m/z* 539.2239, and *m/z* 496.1818)
		Yes	Of carbonyl *N, N*-demethylated compound (*m/z* 538.1924 and *m/z* 524.1769)

negative ionization mode (data not shown).

As a result of the hydroxylation of a doubly N-demethylated product of netupitant, product H (m/z 567.2189) was formed (Fig. 3H), peaking at approximately 1400 mV in the mass voltammogram. Furthermore, product H underwent an additional hydroxylation reaction, forming a doubly hydroxylated, doubly demethylated derivative, m/z 583.2140 (Fig. 3I). With a slightly lower onset at 700 mV and peaking at approximately 1000 mV, m/z 565.2035 was identified, being the result of a mono-hydroxylation reaction on the alkyl side chain of the phenyl ring, followed by its oxidation to a carbonyl moiety of the doubly N-demethylated compound (Fig. 3J). As the second line of oxidation, two additional products emerged at m/z 538.1924 and 524.1769 (Figs. 3K and L), peaking at 1200 and 1500 mV, respectively, having been formed through opening of the piperazine ring of m/z 565.2035 (Fig. 4).

To ascertain whether it is possible to electrochemically mimic the results of another study that had reported the oxidative metabolization of netupitant in vivo [10], several mono- and double-hydroxylated derivatives as well as metabolites from dealkylation, N-oxidation, and piperazine ring-opening reactions were mimicked using our instrumental approach (Fig. 3). As shown in Table 1 [10], which lists the similarities and dissimilarities between the enzyme-mediated and electrochemically mimicked oxidative transformation of netupitant, it can be stated that it is indeed possible to electrochemically simulate the main types of the previously reported oxidation reactions. Nevertheless, we were unable to observe some of the CYP enzyme-mediated reactions known to be involved in the oxidative biotransformation of netupitant [10], namely, the oxidation of carbonyl groups to carboxylic acid. Furthermore, not all electrochemically mimicked oxidation reactions led to the same end-products as those identified in the in vivo biotransformation study [10].

Sum formula annotation of the electrochemically generated oxidation metabolites of netupitant was carried out using the m/z values calculated from the signals detected by EC/LC/MS in ESI(+) mode (SI 4, Table S1). The calculated relative mass deviations were low (< 1 ppm), which alongside the fragmentation spectra (SI 3, Fig. S1) offered strong support for the structural identification of the compounds. Aside from the closest fit of mass accuracy, the process for assigning structures to the recorded high-resolution MS ions was guided by additional criteria, such as former reports on the oxidative biotransformation of netupitant, possible collision-induced dissociation fragmentations or rearrangements of ions during ESI/MS analysis, and other intermediates potentially explaining sequential oxidation processes.

For identification purposes, structural confirmation was also performed using MS/MS fragmentation experiments (data shown in SI 3). A common ion (m/z 522.1975), demonstrating structural relatedness, was generated through several steps of N-dealkylation and piperazine ring opening in the MS/MS fragmentation of netupitant (m/z 579.2551, Fig. 5), along with the dealkylated products m/z 553.2397 and 539.2239 and the N-oxidized species m/z 609.2292 (SI 3, Fig. S1). However, MS/MS fragmentation experiments could not provide further support for the structural allocation of all electrochemically generated species (i.e., the LC-separated isobaric compounds m/z 563.2240); therefore, additional structural elucidation using more advanced analytical tools, such as nuclear magnetic resonance spectroscopy, is needed.

4. Conclusions

Despite the fact that netupitant is routinely used in various therapeutic schemes in combination with other compounds, there is a dearth of available information about its metabolic fate. Although previous studies have suggested the extensive hepatic

metabolization of netupitant and its role as an enzymatic inhibitor, data regarding the structures of the metabolites are lacking. In this study, the use of a non-enzymatic setup for mimicking the oxidative metabolization of netupitant led to the generation of a significant number of oxidation products through various N-dealkylation, N-oxidation, hydroxylation, and piperazine ring-opening processes, adding to the overall picture of the previously unknown electrochemical behavior of this NK_1 receptor antagonist. Additionally, the reversed-phase chromatographic separation of the oxidation products revealed the generation of two isobaric compounds that would have been overlooked by simple EC/MS experiments. The substantial overlap between the previously described CYP-catalyzed metabolites and our electrochemically generated oxidation products may further encourage the in vitro/in vivo pursuit of netupitant metabolites. These products could potentially be correlated with both novel and extensively studied therapeutic applications of this NK_1 receptor antagonist and might be responsible for the reported side effects of unknown origin. Finally, the EC/LC/MS method employed in this study represents a convenient alternative means of generating pure netupitant metabolites in desired amounts for use in future pharmacotoxicological, preclinical, and clinical studies.

Declaration of competing interest

The authors declare that there are no conflicts of interest.

Appendix A. Supplementary data

Supplementary data to this article can be found online at https://doi.org/10.1016/j.jpha.2021.03.011.

References

[1] M. Di Maio, C. Baratelli, P. Bironzo, et al., Efficacy of neurokinin-1 receptor antagonists in the prevention of chemotherapy-induced nausea and vomiting in patients receiving carboplatin-based chemotherapy: a systematic review and meta-analysis, Crit. Rev. Oncol. Hematol. 124 (2018) 21−28.

[2] C. Rojas, M. Raje, T. Tsukamoto, et al., Molecular mechanisms of 5-HT3 and NK1 receptor antagonists in prevention of emesis, Eur. J. Pharmacol. 722 (2014) 26−37.

[3] J.A. Rudd, M.P. Ngan, Z. Lu, et al., Profile of antiemetic activity of netupitant alone or in combination with palonosetron and dexamethasone in ferrets and suncus murinus (house musk shrew), Front. Pharmacol. 7 (2016) 1019−1045.

[4] M. Karthaus, X. Schiel, C.H. Ruhlmann, et al., Neurokinin-1 receptor antagonists: review of their role for the prevention of chemotherapy-induced nausea and vomiting in adults, Expet Rev. Clin. Pharmacol. 12 (2019) 661−680.

[5] S.C. Huang, V.L. Korlipara, Neurokinin-1 receptor antagonists: a comprehensive patent survey, Expert Opin. Ther. Pat. 20 (2010) 1019−1045.

[6] M. Muñoz, R. Coveñas, Involvement of substance P and the NK-1 receptor in human pathology, Amino Acids 46 (2014) 1727−1750.

[7] F. Pertusati, M. Serpi, E. Pileggi, Polyfluorinated scaffolds in drug discovery, in: Fluorine in Life Sciences: Pharmaceuticals, Medicinal Diagnostics, and Agrochemicals, Elsevier B.V., 2019, pp. 141−180.

[8] S. Curran, S. Musa, A. Sajjadi, Hypnosedatives and anxiolytics, in: Side Effects of Drugs Annual, 1st ed., Elsevier B.V., 2015, pp. 57−61.

[9] A. Rizzi, B. Campi, V. Camarda, et al., In vitro and in vivo pharmacological characterization of the novel NK1 receptor selective antagonist Netupitant, Peptides 37 (2012) 86−97.

[10] T. Spinelli, S. Calcagnile, C. Giuliano, et al., Netupitant PET imaging and ADME studies in humans, J. Clin. Pharmacol. 54 (2014) 97−108.

[11] U. Jurva, L. Weidolf, Electrochemical generation of drug metabolites with

applications in drug discovery and development, TrAC-Trend Anal. Chem. (Reference Ed.) 70 (2015) 92–99.

[12] A. Baumann, U. Karst, Online electrochemistry/mass spectrometry in drug metabolism studies: principles and applications, Expet Opin. Drug Metabol. Toxicol. 6 (2010) 715–731.

[13] S. Jahn, U. Karst, Electrochemistry coupled to (liquid chromatography/) mass spectrometry—current state and future perspectives, J. Chromatogr. A 1259 (2012) 16–49.

[14] A. Potęga, D. Żelaszczyk, Z. Mazerska, Electrochemical and in silico approaches for liver metabolic oxidation of antitumor-active triazoloacridinone C-1305, J. Pharm. Anal. 10 (2020) 376–384.

[15] L.M. Frensemeier, L. Büter, M. Vogel, et al., Investigation of the oxidative transformation of roxarsone by electrochemistry coupled to hydrophilic interaction liquid chromatography/mass spectrometry, J. Anal. At. Spectrom. 32 (2017) 153–161.

[16] C. Brauckmann, H. Faber, C. Lanvers-Kaminsky, et al., Influence of cimetidine and its metabolites on Cisplatin—investigation of adduct formation by means of electrochemistry/liquid chromatography/electrospray mass spectrometry, J. Chromatogr. A 1279 (2013) 49–57.

[17] P. Mielczarek, M. Smoluch, J.H. Kotlinska, et al., Electrochemical generation of selegiline metabolites coupled to mass spectrometry, J. Chromatogr. A 1389 (2015) 96–103.

[18] A. Baumann, W. Lohmann, B. Schubert, et al., Metabolic studies of tetrazepam based on electrochemical simulation in comparison to in vivo and in vitro methods, J. Chromatogr. A 1216 (2009) 3192–3198.

[19] W. Lohmann, U. Karst, Biomimetic modeling of oxidative drug metabolism, Anal. Bioanal. Chem. 391 (2008) 79–96.

[20] U. Jurva, H.V. Wikström, L. Weidolf, et al., Comparison between electrochemistry/mass spectrometry and cytochrome P450 catalyzed oxidation reactions, Rapid Commun. Mass Spectrom. 17 (2003) 800–810.

[21] K. Sandoval, K. Witt, Gastrointestinal drugs, in: Side Effects of Drugs Annual, 1st ed., Elsevier B.V., 2015, pp. 433–459.

[22] R.M. Umar, Drug-drug interactions between antiemetics used in cancer patients, J. Oncol. Sci. 4 (2018) 142–146.

[23] S. Hanessian, V. Babonneau, N. Boyer, et al., Design and synthesis of potential dual NK1/NK3 receptor antagonists, Bioorg. Med. Chem. Lett 24 (2014) 510–514.